

Blind Deconvolution with Non-smooth Regularization via Bregman Proximal DCAs

Shota Takahashi, Mirai Tanaka, and Shiro Ikeda, *Member, IEEE*

Abstract—Blind deconvolution is a technique to recover an original signal without knowing a convolving filter. It is naturally formulated as a minimization of a quartic objective function under some assumption. Because its differentiable part does not have a Lipschitz continuous gradient, existing first-order methods are not theoretically supported. In this letter, we employ the Bregman-based proximal methods, whose convergence is theoretically guaranteed under the L -smad property. We first reformulate the objective function as a difference of convex (DC) functions and apply the Bregman proximal DC algorithm (BPDCA). This DC decomposition satisfies the L -smad property. The method is extended to the BPDCA with extrapolation (BPDCAe) for faster convergence. When our regularizer has a sufficiently simple structure, each iteration is solved in a closed-form expression, and thus our algorithms solve large-scale problems efficiently. We also provide the stability analysis of the equilibriums and demonstrate the proposed methods through numerical experiments on image deblurring. The results show that BPDCAe successfully recovered the original image and outperformed other existing algorithms.

Index Terms—Blind deconvolution, DC optimization, Bregman proximal DC algorithms, image deblurring.

I. INTRODUCTION

WE consider the convolution of a filter $\mathbf{f} \in \mathbb{R}^m$ and a signal $\mathbf{g} \in \mathbb{R}^m$, given by

$$\tilde{\mathbf{y}} = \mathbf{f} * \mathbf{g}. \quad (1)$$

Our goal is to recover \mathbf{g} from $\tilde{\mathbf{y}}$ without knowing \mathbf{f} . This problem is known as blind deconvolution. Blind deconvolution arises in many fields of science and engineering, such as sensor networks [2], optics [7], astronomy [8], [9], communication engineering [12], and medical image processing [15].

Without any assumptions, blind deconvolution is ill-posed. A common approach is to assume that \mathbf{f} and \mathbf{g} belong to known subspaces [1]. For known linear operators $\tilde{\mathbf{B}} : \mathbb{R}^{d_1} \rightarrow \mathbb{R}^m$ and $\tilde{\mathbf{A}} : \mathbb{R}^{d_2} \rightarrow \mathbb{R}^m$, we assume that there exist $\mathbf{h}^* \in \mathbb{R}^{d_1}$ and $\mathbf{x}^* \in \mathbb{R}^{d_2}$ such that $\mathbf{f} = \tilde{\mathbf{B}}\mathbf{h}^*$ and $\mathbf{g} = \tilde{\mathbf{A}}\mathbf{x}^*$, where $d_1, d_2 < m$. Let $\mathbf{F} \in \mathbb{C}^{m \times m}$ be the unitary discrete Fourier transform (DFT) matrix. Multiplying $\sqrt{m}\mathbf{F}$ on both sides of (1), $\sqrt{m}\mathbf{F}\tilde{\mathbf{y}} = m\mathbf{F}\tilde{\mathbf{B}}\mathbf{h}^* \odot \mathbf{F}\tilde{\mathbf{A}}\mathbf{x}^*$ holds, where \odot denotes

the Hadamard (elementwise) product. Thus, (1) is rewritten in the Fourier domain as $\mathbf{y} = \mathbf{B}\mathbf{h}^* \odot \overline{\mathbf{A}\mathbf{x}^*}$, where $\mathbf{y} := \frac{1}{\sqrt{m}}\mathbf{F}\tilde{\mathbf{y}}$, $\mathbf{B} := \mathbf{F}\tilde{\mathbf{B}}$, and $\overline{\mathbf{A}} := \mathbf{F}\tilde{\mathbf{A}}$.

Now, the goal of our problem is to obtain \mathbf{h} and \mathbf{x} from \mathbf{y} . It is natural to evaluate the fidelity, and we consider the squared error function $F(\mathbf{h}, \mathbf{x}) = \frac{1}{2}\|\mathbf{B}\mathbf{h} \odot \overline{\mathbf{A}\mathbf{x}} - \mathbf{y}\|_2^2$. This is a nonconvex quartic function with respect to (\mathbf{h}, \mathbf{x}) . In this letter, we consider the following optimization problem:

$$\min_{(\mathbf{h}, \mathbf{x}) \in \text{cl } C} F(\mathbf{h}, \mathbf{x}) + G(\mathbf{h}, \mathbf{x}), \quad (2)$$

where $G : \mathbb{R}^{d_1+d_2} \rightarrow (-\infty, +\infty]$ is a regularization term that may not be differentiable, including ℓ_1 norm and total variation, and $C \subset \mathbb{R}^{d_1+d_2}$ is a nonempty open convex set. Because F is quartic and does not have a Lipschitz continuous gradient, we cannot rely on the convergence analysis of existing first order methods, such as the fast iterative shrinkage-thresholding algorithm (FISTA) [3]. Instead, we try to resort to Bregman-based proximal gradient algorithms [4]. These algorithms generalize the proximal gradient method by replacing the squared Euclidean distance with the Bregman distance D_H associated with a kernel generating distance H . The algorithms generates a sequence converging to a stationary point under the L -smooth adaptable (L -smad) property of (F, H) defined later. For our problem, however, finding an appropriate H is difficult because of the bilinear term of F .

To address the problem, we first reformulate F into a difference of convex (DC) functions and apply the Bregman proximal DC algorithm (BPDCA) [14]. For our DC decomposition $F = F_1 - F_2$, we find an H that makes (F_1, H) L -smad, and hence BPDCA with corresponding D_H converges to a stationary point of (2). We also apply a variant, the BPDCA with extrapolation (BPDCAe) [14], which converges faster. When G has a simple structure, each iteration of BPDCA(e) is solved in a closed form. This fact implies that our algorithms solve large-scale problems efficiently. We also show the stability property of the algorithms around the equilibriums and compare them with existing algorithms. Moreover, we show a numerical example of image deblurring.

Notation: Vectors and matrices are shown in boldface. All one vector is $\mathbf{1} \in \mathbb{R}^m$ and the identity matrix is $\mathbf{I}_d \in \mathbb{R}^{d \times d}$. Let $|z|$ and z^2 be elementwise absolute and squared vectors for $\mathbf{z} \in \mathbb{C}^d$, respectively. $\text{Re}(\mathbf{z})$, $\bar{\mathbf{z}}$, and \mathbf{z}^H denote its real part, complex conjugate, and complex conjugate transpose, respectively. The inner product of $\mathbf{z}, \mathbf{w} \in \mathbb{C}^d$ is defined by $\langle \mathbf{z}, \mathbf{w} \rangle = \mathbf{z}^H \mathbf{w}$.

This work has been submitted to the IEEE for possible publication. Copyright may be transferred without notice, after which this version may no longer be accessible.

Manuscript received May 16, 2022; revised 2022.

S. Takahashi is with the Department of Statistical Science, the Graduate University for Advanced Studies, 10–3 Midori-cho, Tachikawa, Tokyo 190–8562, Japan (e-mail: takahashi.shota@ism.ac.jp).

M. Tanaka and S. Ikeda are with the Department of Statistical Inference and Mathematics, the Institute of Statistical Mathematics, 10–3 Midori-cho, Tachikawa, Tokyo 190–8562, Japan (e-mail: mirai@ism.ac.jp; shiro@ism.ac.jp).

M. Tanaka is also with Continuous Optimization Team, RIKEN Center for Advanced Intelligence Project.

Algorithm 1 BPDCA [14] for DC optimization problem (3)

Input: $H \in \mathcal{G}(C)$, $\mathbf{z}^0 \in C$ and $0 < \lambda < 1/L$.
for $k = 0, 1, 2, \dots$, **do**

$$\mathbf{z}^{k+1} = \underset{\mathbf{z} \in \text{cl } C}{\text{argmin}} \{ \langle \nabla F_1(\mathbf{z}^k) - \nabla F_2(\mathbf{z}^k), \mathbf{z} \rangle + G(\mathbf{z}) + \frac{1}{\lambda} D_H(\mathbf{z}, \mathbf{z}^k) \}. \quad (4)$$

II. PROPOSED METHOD

A. DC Decomposition

We first reformulate F in (2) into a DC function. Let us define F_1 and F_2 as follows:

$$F_1(\mathbf{h}, \mathbf{x}) = \frac{1}{4} \|\mathbf{B}\mathbf{h}\|_4^4 + \frac{1}{4} \|\mathbf{A}\mathbf{x}\|_4^4 + \frac{1}{2} (\|\mathbf{B}\mathbf{h} \odot \mathbf{A}\mathbf{x}\|_2^2 + \|\mathbf{y} \odot \mathbf{B}\mathbf{h}\|_2^2 + \|\mathbf{A}\mathbf{x}\|_2^2 + \|\mathbf{y}\|_2^2),$$

$$F_2(\mathbf{h}, \mathbf{x}) = \frac{1}{4} \|\mathbf{B}\mathbf{h}\|_4^4 + \frac{1}{4} \|\mathbf{A}\mathbf{x}\|_4^4 + \frac{1}{2} \|\bar{\mathbf{y}} \odot \mathbf{B}\mathbf{h} + \overline{\mathbf{A}\mathbf{x}}\|_2^2.$$

F_2 is obviously convex. By denoting \mathbf{b}_j and \mathbf{a}_j be the j -th column vectors of \mathbf{B}^H and \mathbf{A}^H , respectively, we have $F_1(\mathbf{h}, \mathbf{x}) = \frac{1}{4} \sum_{j=1}^m (|\mathbf{b}_j^H \mathbf{h}|^2 + |\mathbf{a}_j^H \mathbf{x}|^2)^2 + \frac{1}{2} (\|\mathbf{y} \odot \mathbf{B}\mathbf{h}\|_2^2 + \|\mathbf{A}\mathbf{x}\|_2^2 + \|\mathbf{y}\|_2^2)$, which proves the convexity of F_1 . Since $F = F_1 - F_2$ holds, (2) is equivalent to the following DC optimization problem:

$$\min_{\{\mathbf{h}, \mathbf{x}\}^T \in \text{cl } C} F_1(\mathbf{h}, \mathbf{x}) - F_2(\mathbf{h}, \mathbf{x}) + G(\mathbf{h}, \mathbf{x}). \quad (3)$$

B. Bregman Proximal DC Algorithms

Before showing DC algorithms, we define the kernel generating distances, the Bregman distances, and the L -smooth adaptable property.

Definition 1 (Kernel Generating Distances [4] and Bregman Distances [5]): Let C be a nonempty open convex subset of \mathbb{R}^d . $H : \mathbb{R}^d \rightarrow (-\infty, +\infty]$ is called a kernel generating distance associated with C if it meets the following conditions:

- (i) H is proper, lower semicontinuous, and convex, with $\text{dom } H \subset \text{cl } C$ and $\text{dom } \partial H = C$.
- (ii) H is \mathcal{C}^1 on $\text{int dom } H = C$.

We denote the class of the kernel generating distances associated with C by $\mathcal{G}(C)$. Given $H \in \mathcal{G}(C)$, the Bregman distance $D_H : \text{dom } H \times \text{int dom } H \rightarrow \mathbb{R}_+$ is defined by $D_H(\mathbf{z}, \mathbf{w}) := H(\mathbf{z}) - H(\mathbf{w}) - \langle \nabla H(\mathbf{w}), \mathbf{z} - \mathbf{w} \rangle$.

Definition 2 (L-smooth adaptable (L-smad) [4]): Consider a pair of functions (F, H) satisfying the following conditions:

- (i) $H \in \mathcal{G}(C)$,
- (ii) $F : \mathbb{R}^d \rightarrow (-\infty, +\infty]$ is proper, lower semicontinuous, and \mathcal{C}^1 on $C = \text{int dom } H$ with $\text{dom } F \supset \text{dom } H$.

The pair (F, H) is called L -smooth adaptable (L -smad) on C if there exists $L > 0$ such that $LH - F$ and $LH + F$ are convex on C .

To solve (3), we introduce the Bregman proximal DC algorithm (BPDCA) [14] in Algorithm 1 and the BPDCA with extrapolation (BPDCAe) [14] in Algorithm 2, where we denoted $\mathbf{z} = (\mathbf{h}, \mathbf{x})$. The function G is possibly non-smooth,

Algorithm 2 BPDCAe [14] for DC optimization problem (3)

Input: $H \in \mathcal{G}(C)$, $\mathbf{z}^{-1} = \mathbf{z}^0 \in C$, $t_{-1} = t_0 = 1$,
 $0 < \lambda < 1/L$, $\rho \in [0, 1)$, and $K \in \mathbb{N}$.

for $k = 0, 1, 2, \dots$, **do**

$$\mathbf{w}^k = \mathbf{z}^k + \frac{t_{k-1}-1}{t_k} (\mathbf{z}^k - \mathbf{z}^{k-1}), \quad t_{k+1} = \frac{1 + \sqrt{1 + 4t_k^2}}{2}.$$

if $k = nK$ with $n \in \mathbb{N}$, $\mathbf{w}^k \notin C$, or
 $D_H(\mathbf{z}^k, \mathbf{w}^k) > \rho D_H(\mathbf{z}^{k-1}, \mathbf{z}^k)$ **then**
 $t_{k-1} = t_k = 1$ and $\mathbf{w}^k = \mathbf{z}^k$.

$$\mathbf{z}^{k+1} = \underset{\mathbf{z} \in \text{cl } C}{\text{argmin}} \{ \langle \nabla F_1(\mathbf{w}^k) - \nabla F_2(\mathbf{z}^k), \mathbf{z} \rangle + G(\mathbf{z}) + \frac{1}{\lambda} D_H(\mathbf{z}, \mathbf{w}^k) \}. \quad (5)$$

and when G has a sufficiently simple structure, (4) and (5) are easily solved. For instance, we solve subproblem (4) to obtain the sparse signal and filter when $G(\mathbf{h}, \mathbf{x}) = \theta_1 \|\mathbf{h}\|_1 + \theta_2 \|\mathbf{x}\|_1$ for $\theta_1, \theta_2 \geq 0$. Let $\mathbf{u} = \mathcal{S}_{\lambda\theta_1}(\lambda \nabla_{\mathbf{h}} F(\mathbf{z}^k) - \nabla_{\mathbf{h}} H(\mathbf{z}^k))$ and $\mathbf{v} = \mathcal{S}_{\lambda\theta_2}(\lambda \nabla_{\mathbf{x}} F(\mathbf{z}^k) - \nabla_{\mathbf{x}} H(\mathbf{z}^k))$, where \mathcal{S}_τ is the soft-thresholding operator [4] with $\tau > 0$. We can prove from [4, Proposition 5.1] that $\mathbf{z}^{k+1} = (-t^* \mathbf{u}, -t^* \mathbf{v})$ solves subproblem (4), where t^* is the unique positive real root of the cubic equation $t^3 (\|\mathbf{u}\|_2^2 + \|\mathbf{v}\|_2^2) + t - 1 = 0$. Note that every cubic equation has a closed-form solution via Cardano's formula. This fact indicates solution of (4) is expressed in closed form. It is also true for subproblem (5). When (F_1, H) is L -smad, the convergence of the algorithms to a stationary point is guaranteed [14]. In theory and practice, BPDCAe converges faster than BPDCA [14], whereas BPDCAe requires the convexity of G .

The following theorem provides appropriate H and L in use of Algorithms 1 and 2.

Theorem 1: Let H be defined by

$$H(\mathbf{h}, \mathbf{x}) = \frac{1}{4} (\|\mathbf{h}\|_2^2 + \|\mathbf{x}\|_2^2)^2 + \frac{1}{2} (\|\mathbf{h}\|_2^2 + \|\mathbf{x}\|_2^2). \quad (6)$$

Then, for any L satisfying

$$L \geq \sum_{j=1}^m (3\|\mathbf{b}_j\|_2^4 + 3\|\mathbf{a}_j\|_2^4 + \|\mathbf{b}_j\|_2^2 \|\mathbf{a}_j\|_2^2 + |\mathbf{y}_j|^2 \|\mathbf{b}_j\|_2^2 + \|\mathbf{a}_j\|_2^2), \quad (7)$$

the function $LH - F_1$ is convex on $\mathbb{R}^{d_1+d_2}$.

Proof: We obtain the Hessian of H and F_1 as follows:

$$\nabla^2 H(\mathbf{z}) = (\|\mathbf{z}\|_2^2 + 1) \mathbf{I}_{d_1+d_2} + 2\mathbf{z}\mathbf{z}^T,$$

$$\nabla^2 F_1(\mathbf{h}, \mathbf{x}) = \text{Re} \begin{bmatrix} \mathbf{H}_{11} & \mathbf{H}_{12} \\ \mathbf{H}_{12}^T & \mathbf{H}_{22} \end{bmatrix},$$

where $\mathbf{z} = (\mathbf{h}, \mathbf{x}) \in \mathbb{R}^{d_1+d_2}$ and

$$\mathbf{H}_{11} := \mathbf{B}^H \text{diag}(2|\mathbf{B}\mathbf{h}|^2 + |\mathbf{A}\mathbf{x}|^2 + |\mathbf{y}|^2) \mathbf{B} + \mathbf{B}^H \text{diag}((\mathbf{B}\mathbf{h})^2) \bar{\mathbf{B}},$$

$$\mathbf{H}_{12} := \mathbf{B}^H \text{diag}(\mathbf{B}\mathbf{h} \odot \mathbf{A}\mathbf{x}) \bar{\mathbf{A}} + \mathbf{B}^H \text{diag}(\mathbf{B}\mathbf{h} \odot \overline{\mathbf{A}\mathbf{x}}) \mathbf{A},$$

$$\mathbf{H}_{22} := \mathbf{A}^H \text{diag}(|\mathbf{B}\mathbf{h}|^2 + 2|\mathbf{A}\mathbf{x}|^2 + 1) \mathbf{A} + \mathbf{A}^H \text{diag}((\mathbf{A}\mathbf{x})^2) \bar{\mathbf{A}}.$$

Since the sum of a complex number and its conjugate is real, $\nabla^2 F_1$ is real. To prove the convexity of $LH - F_1$, it is sufficient to show that $\langle \mathbf{w}, \nabla^2 F_1(\mathbf{h}, \mathbf{x}) \mathbf{w} \rangle \leq L \langle \mathbf{w}, \nabla^2 H(\mathbf{h}, \mathbf{x}) \mathbf{w} \rangle$ for any $\mathbf{w} \in \mathbb{R}^{d_1+d_2}$. Let separate $\mathbf{w} = (\mathbf{u}, \mathbf{v})$ using $\mathbf{u} \in \mathbb{R}^{d_1}$ and $\mathbf{v} \in \mathbb{R}^{d_2}$. We obtain $\langle \mathbf{w}, \nabla^2 H(\mathbf{z}) \mathbf{w} \rangle = (\|\mathbf{z}\|_2^2 + 1) \|\mathbf{w}\|_2^2 + 2\langle \mathbf{z}, \mathbf{w} \rangle^2$ and

$$\begin{aligned} & \langle \mathbf{w}, \nabla^2 F_1(\mathbf{h}, \mathbf{x}) \mathbf{w} \rangle \\ &= \text{Re} \langle \mathbf{u}, \mathbf{H}_{11} \mathbf{u} \rangle + \text{Re} \langle \mathbf{v}, \mathbf{H}_{22} \mathbf{v} \rangle + 2 \text{Re} \langle \mathbf{u}, \mathbf{H}_{12} \mathbf{v} \rangle. \end{aligned}$$

Each term of $\langle \mathbf{w}, \nabla^2 F_1(\mathbf{h}, \mathbf{x}) \mathbf{w} \rangle$ is bounded as follows:

$$\begin{aligned} & \text{Re} \langle \mathbf{u}, \mathbf{H}_{11} \mathbf{u} \rangle \\ &= \langle 2|\mathbf{Bh}|^2 + |\mathbf{Ax}|^2 + |\mathbf{y}|^2, |\mathbf{Bu}|^2 \rangle + \text{Re} \langle (\mathbf{Bu})^2, (\mathbf{Bh})^2 \rangle \\ &\leq \langle |\mathbf{Bh}|^2 + |\mathbf{Ax}|^2 + |\mathbf{y}|^2, |\mathbf{Bu}|^2 \rangle + 2\langle |\mathbf{Bh}|^2, |\mathbf{Bu}|^2 \rangle, \\ & \text{Re} \langle \mathbf{v}, \mathbf{H}_{22} \mathbf{v} \rangle \\ &= \langle |\mathbf{Bh}|^2 + 2|\mathbf{Ax}|^2 + \mathbf{1}, |\mathbf{Av}|^2 \rangle + \text{Re} \langle (\mathbf{Av})^2, (\mathbf{Ax})^2 \rangle \\ &\leq \langle |\mathbf{Bh}|^2 + |\mathbf{Ax}|^2 + \mathbf{1}, |\mathbf{Av}|^2 \rangle + 2\langle |\mathbf{Ax}|^2, |\mathbf{Av}|^2 \rangle, \\ & \text{Re} \langle \mathbf{u}, \mathbf{H}_{12} \mathbf{v} \rangle \\ &= \text{Re} \langle \mathbf{Bu} \odot \mathbf{Av}, \mathbf{Bh} \odot \mathbf{Ax} \rangle + \text{Re} \langle \mathbf{Bu} \odot \overline{\mathbf{Av}}, \mathbf{Bh} \odot \overline{\mathbf{Ax}} \rangle \\ &\leq 2 \sum_{j=1}^m \|\mathbf{b}_j\|_2^2 \|\mathbf{a}_j\|_2^2 \|\mathbf{h}\|_2 \|\mathbf{u}\|_2 \|\mathbf{x}\|_2 \|\mathbf{v}\|_2, \end{aligned}$$

where the first and second inequalities hold by $\text{Re}(\cdot) \leq |\cdot|$, and the last inequality holds by the Cauchy-Schwarz inequality. From the above relation, we obtain

$$\begin{aligned} & \langle |\mathbf{Bh}|^2, |\mathbf{Bu}|^2 \rangle + \langle |\mathbf{Ax}|^2, |\mathbf{Av}|^2 \rangle + \text{Re} \langle \mathbf{u}, \mathbf{H}_{12} \mathbf{v} \rangle \\ &\leq \sum_{j=1}^m (\|\mathbf{b}_j\|_2^4 \|\mathbf{h}\|_2^2 \|\mathbf{u}\|_2^2 + \|\mathbf{a}_j\|_2^4 \|\mathbf{x}\|_2^2 \|\mathbf{v}\|_2^2 \\ &\quad + 2\|\mathbf{b}_j\|_2^2 \|\mathbf{a}_j\|_2^2 \|\mathbf{h}\|_2 \|\mathbf{u}\|_2 \|\mathbf{x}\|_2 \|\mathbf{v}\|_2) \\ &= \sum_{j=1}^m (\|\mathbf{b}_j\|_2^2 \|\mathbf{h}\|_2 \|\mathbf{u}\|_2 + \|\mathbf{a}_j\|_2^2 \|\mathbf{x}\|_2 \|\mathbf{v}\|_2)^2 \\ &\leq \sum_{j=1}^m (\|\mathbf{b}_j\|_2^4 + \|\mathbf{a}_j\|_2^4) (\|\mathbf{h}\|_2^2 \|\mathbf{u}\|_2^2 + \|\mathbf{x}\|_2^2 \|\mathbf{v}\|_2^2), \end{aligned}$$

where both inequalities hold by the Cauchy-Schwarz inequality. Thus, we obtain

$$\begin{aligned} & \langle \mathbf{w}, \nabla^2 F_1(\mathbf{h}, \mathbf{x}) \mathbf{w} \rangle \\ &\leq \langle |\mathbf{Bh}|^2 + |\mathbf{Ax}|^2 + |\mathbf{y}|^2, |\mathbf{Bu}|^2 \rangle \\ &\quad + \langle |\mathbf{Bh}|^2 + |\mathbf{Ax}|^2 + \mathbf{1}, |\mathbf{Av}|^2 \rangle \\ &\quad + 2\langle |\mathbf{Bh}|^2, |\mathbf{Bu}|^2 \rangle + 2\langle |\mathbf{Ax}|^2, |\mathbf{Av}|^2 \rangle + 2 \text{Re} \langle \mathbf{u}, \mathbf{H}_{12} \mathbf{v} \rangle \\ &\leq \sum_{j=1}^m (\|\mathbf{b}_j\|_2^2 \|\mathbf{u}\|_2^2 (\|\mathbf{b}_j\|_2^2 \|\mathbf{h}\|_2^2 + \|\mathbf{a}_j\|_2^2 \|\mathbf{x}\|_2^2 + |\mathbf{y}_j|^2) \\ &\quad + \|\mathbf{a}_j\|_2^2 \|\mathbf{v}\|_2^2 (\|\mathbf{b}_j\|_2^2 \|\mathbf{h}\|_2^2 + \|\mathbf{a}_j\|_2^2 \|\mathbf{x}\|_2^2 + 1) \\ &\quad + 2(\|\mathbf{b}_j\|_2^4 + \|\mathbf{a}_j\|_2^4) (\|\mathbf{h}\|_2^2 \|\mathbf{u}\|_2^2 + \|\mathbf{x}\|_2^2 \|\mathbf{v}\|_2^2)) \\ &\leq \sum_{j=1}^m (3\|\mathbf{b}_j\|_2^4 + 3\|\mathbf{a}_j\|_2^4 + \|\mathbf{b}_j\|_2^2 \|\mathbf{a}_j\|_2^2 \\ &\quad + |\mathbf{y}_j|^2 \|\mathbf{b}_j\|_2^2 + \|\mathbf{a}_j\|_2^2) (\|\mathbf{z}\|_2^2 + 1) \|\mathbf{w}\|_2^2 \\ &\leq L \langle \mathbf{w}, \nabla^2 H(\mathbf{h}, \mathbf{x}) \mathbf{w} \rangle, \end{aligned}$$

which proves $LH - F_1$ is convex.

From Theorem 1, we obtain the following (proofs are omitted).

Corollary 1: Let $H_C \in \mathcal{G}(C)$ be defined by $H_C(\mathbf{z}) = \frac{1}{4} \|\mathbf{z}\|_2^4 + \frac{1}{2} \|\mathbf{z}\|_2^2 + \delta_C(\mathbf{z})$, where $\delta_C(\mathbf{z})$ is the indicator function $\delta_C(\mathbf{z}) = 0$ for $\mathbf{z} \in C$ and $\delta_C(\mathbf{z}) = \infty$ otherwise. For any L satisfying (7), the pair (F_1, H_C) is L -smad on C .

From Corollary 1, we can immediately prove the following corollary by using [14, Theorems 2 and 7].

Corollary 2: Let $\{\mathbf{z}^k\}$ be a sequence generated by BPDCA(e) with $0 < \lambda L < 1$ for (3). For BPDCAe, assume G is convex. Then, $\{\mathbf{z}^k\}$ converges to a stationary point of (3). Note that a stationary point of (3) is defined as a point $\mathbf{z} \in C$ satisfying $-\nabla F_1(\mathbf{z}) + \nabla F_2(\mathbf{z}) \in \partial G(\mathbf{z})$, where ∂G denotes the limiting subdifferential of G defined in [14, Definition 5], which coincides with the subdifferential of G under the convexity. Note that under the convexity of G , it is theoretically guaranteed that a sequence generated by FISTA would converge to the stationary point if F had a Lipschitz continuous gradient. In our problem, the convergence of FISTA is not theoretically guaranteed because F does not have it. Although FISTA is not applicable, the convergent points of BPDCA(e) and FISTA share the same stationary points in theory.

C. Stability Analysis

We show the stability analysis of BPDCA(e), FISTA, and the alternating minimization (AM) [6], [10], [13] around the equilibrium points. Here, we define $\Phi(\mathbf{z}) = G(\mathbf{z}) + \langle \nabla F(\mathbf{z}^k), \mathbf{z} \rangle + \frac{1}{\lambda} D_H(\mathbf{z}, \mathbf{z}^k)$. Then, the first-order condition $\mathbf{0} \in \partial \Phi(\mathbf{z}^{k+1}) = \partial G(\mathbf{z}^{k+1}) + \nabla F(\mathbf{z}^k) + \frac{1}{\lambda} (\nabla H(\mathbf{z}^{k+1}) - \nabla H(\mathbf{z}^k))$ is approximated as follows:

$$\mathbf{0} \simeq \zeta^{k+1} + \nabla F(\mathbf{z}^k) + \frac{1}{\lambda} \nabla^2 H(\mathbf{z}^k) (\mathbf{z}^{k+1} - \mathbf{z}^k),$$

where $\zeta^{k+1} \in \partial G(\mathbf{z}^{k+1})$. Because $\nabla^2 H(\mathbf{z}^k)$ is regular, we obtain

$$\mathbf{z}^{k+1} - \mathbf{z}^k \simeq -\lambda \nabla^2 H(\mathbf{z}^k)^{-1} (\zeta^{k+1} + \nabla F(\mathbf{z}^k)),$$

which indicates that $\mathbf{z}^{k+1} - \mathbf{z}^k$ is greatly affected by $\nabla^2 H(\mathbf{z})^{-1} = \frac{1}{\|\mathbf{z}\|_2^2 + 1} \left(\mathbf{I}_{d_1+d_2} - \frac{2\mathbf{z}\mathbf{z}^\top}{3\|\mathbf{z}\|_2^2 + 1} \right)$. Thus, H is important for the performance of BPDCA. For BPDCAe, this fact is also true by substituting \mathbf{w}^k for \mathbf{z}^k .

To simplify the stability analysis of FISTA, we consider ISTA, which is FISTA without extrapolation. Setting $H(\mathbf{z}) = \frac{1}{2} \|\mathbf{z}\|_2^2 =: H_1(\mathbf{z})$, i.e., $\nabla^2 H_1(\mathbf{z}) = \mathbf{I}_{d_1+d_2}$, we obtain

$$\mathbf{z}^{k+1} - \mathbf{z}^k \simeq -\lambda (\zeta^{k+1} + \nabla F(\mathbf{z}^k)).$$

Since F does not have a Lipschitz continuous gradient, λ is close to 0, i.e., $\mathbf{z}^k \simeq \mathbf{z}^{k+1}$. This implies that convergence of (F)ISTA is slow.

When $G(\mathbf{x}, \mathbf{h})$ is convex, (2) is convex with respect to \mathbf{h} for fixed \mathbf{x} and vice versa. AM is a method to update \mathbf{x} and \mathbf{h} alternately, which will be easily implemented and converge. The first-order conditions around the equilibrium points are

$$\begin{aligned} & \mathbf{0} \in \partial_{\mathbf{h}} G(\mathbf{h}^{k+1}, \mathbf{x}^k) + \nabla_{\mathbf{h}} F(\mathbf{h}^{k+1}, \mathbf{x}^k) \\ & \quad \simeq \partial_{\mathbf{h}} G(\mathbf{h}^{k+1}, \mathbf{x}^k) + \nabla_{\mathbf{h}} F(\mathbf{h}^k, \mathbf{x}^k) + \mathbf{M}_{\mathbf{h}}(\mathbf{h}^{k+1} - \mathbf{h}^k), \\ \blacksquare & \quad \mathbf{0} \in \partial_{\mathbf{x}} G(\mathbf{h}^{k+1}, \mathbf{x}^{k+1}) + \nabla_{\mathbf{x}} F(\mathbf{h}^{k+1}, \mathbf{x}^{k+1}) \end{aligned}$$

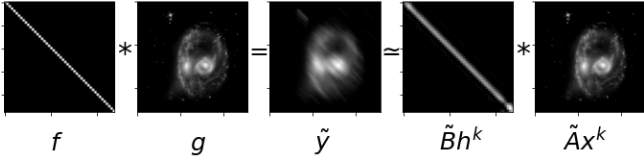


Fig. 1. The ground truth \mathbf{f} and \mathbf{g} , the blurred image $\tilde{\mathbf{y}}$, and $\tilde{\mathbf{B}}\mathbf{h}^k$ and $\tilde{\mathbf{A}}\mathbf{x}^k$ recovered by BPDCAe.

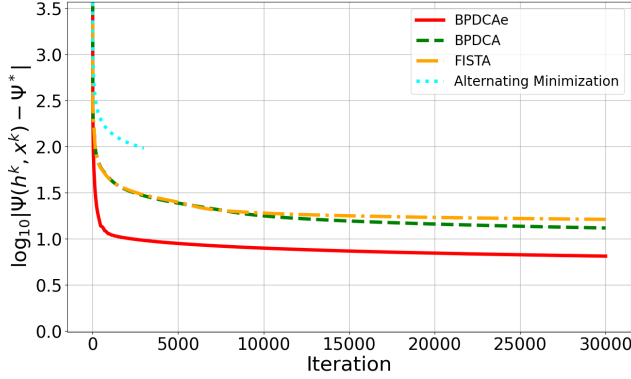


Fig. 2. Plots of $\log_{10} |\Psi(\mathbf{h}^k, \mathbf{x}^k) - \Psi^*|$ at each iteration.

$$\simeq \partial_{\mathbf{x}}G(\mathbf{h}^{k+1}, \mathbf{x}^{k+1}) + \nabla_{\mathbf{x}}F(\mathbf{h}^{k+1}, \mathbf{x}^k) + \mathbf{M}_{\mathbf{x}}(\mathbf{x}^{k+1} - \mathbf{x}^k),$$

where $\mathbf{M}_{\mathbf{h}} = \nabla_{\mathbf{h}\mathbf{h}}^2 F(\mathbf{h}^k, \mathbf{x}^k)$, $\mathbf{M}_{\mathbf{x}} = \nabla_{\mathbf{x}\mathbf{x}}^2 F(\mathbf{h}^k, \mathbf{x}^k)$, and the last approximation holds from $\mathbf{h}^{k+1} \simeq \mathbf{h}^k$ in $\mathbf{M}_{\mathbf{x}}$. For $\zeta_{\mathbf{h}}^{k+1} \in \partial_{\mathbf{h}}G(\mathbf{h}^{k+1}, \mathbf{x}^k)$ and $\zeta_{\mathbf{x}}^{k+1} \in \partial_{\mathbf{x}}G(\mathbf{h}^{k+1}, \mathbf{x}^{k+1})$, we obtain

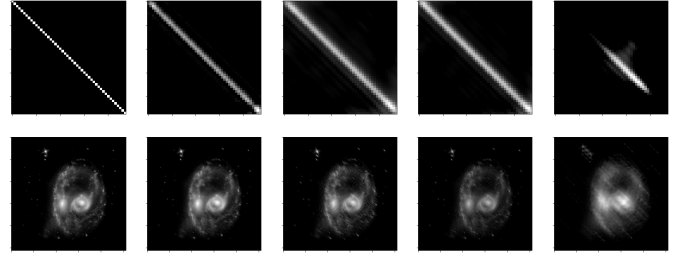
$$\begin{aligned} \mathbf{h}^{k+1} - \mathbf{h}^k &\simeq -\mathbf{M}_{\mathbf{h}}^{-1}(\zeta_{\mathbf{h}}^{k+1} + \nabla_{\mathbf{h}}F(\mathbf{h}^k, \mathbf{x}^k)), \\ \mathbf{x}^{k+1} - \mathbf{x}^k &\simeq -\mathbf{M}_{\mathbf{x}}^{-1}(\zeta_{\mathbf{x}}^{k+1} + \nabla_{\mathbf{x}}F(\mathbf{h}^{k+1}, \mathbf{x}^k)). \end{aligned}$$

Because $\mathbf{M}_{\mathbf{h}}$ and $\mathbf{M}_{\mathbf{x}}$ are not always regular matrices, AM might be unstable. In addition, the equilibrium point by AM may be different from the stationary point of (2). It is demonstrated in numerical experiments (Figure 3).

III. NUMERICAL EXPERIMENTS

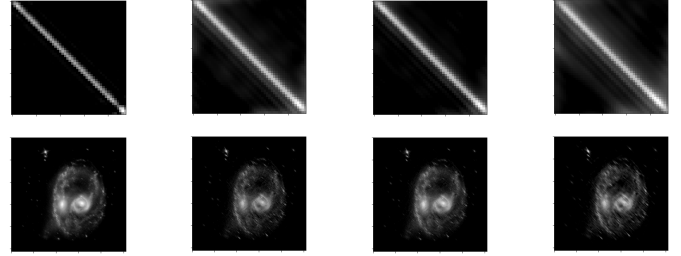
We demonstrated efficiency of our proposed method by image deblurring via solving problem (2). We set $d_1 = 2304$, $d_2 = 65536$, and $m = 262144$ and appropriately took a ground truth of $(\mathbf{h}^*, \mathbf{x}^*)$. Using them, we generated a blurring kernel $\mathbf{f} = \tilde{\mathbf{B}}\mathbf{h}^*$ and an original image $\mathbf{g} = \tilde{\mathbf{A}}\mathbf{x}^*$, where $\tilde{\mathbf{B}} : \mathbb{R}^{d_1} \rightarrow \mathbb{R}^m$ is an operator reshaping $\mathbf{h} \in \mathbb{R}^{d_1}$ into a $\sqrt{m} \times \sqrt{m}$ image and $\tilde{\mathbf{A}} : \mathbb{R}^{d_2} \rightarrow \mathbb{R}^m$ is an inverse discrete Meyer wavelet transform operator. Figure 1 depicts \mathbf{f} and \mathbf{g} used in our experiments: \mathbf{f} corresponds to a diagonal blurring and \mathbf{g} approximates a natural image. We also set $\mathcal{C} = \{(\mathbf{h}, \mathbf{x}) \in \mathbb{R}^{d_1} \times \mathbb{R}^{d_2} \mid \mathbf{h} > \mathbf{0}, \mathbf{x} > \mathbf{0}\}$ and $G(\mathbf{h}, \mathbf{x}) = \theta \|\mathbf{h}\|_1$ with $\theta = 0.01$ (the non-smooth ℓ_1 regularizer) because \mathbf{h} is supposed to be sparse in practice of image deblurring.

We solved problem (2) corresponding to the setting above with BPDCA(e), FISTA, and AM. For BPDCA(e), we adjusted L which satisfies (7) and used it as a fixed step size. Step sizes in all iterations of FISTA were obtained by backtracking. The maximum number of iterations for BPDCA(e) and FISTA was



(a) \mathbf{h}^k and \mathbf{x}^k (b) BPDCAe (c) BPDCA (d) FISTA (e) AM

Fig. 3. The upper row shows \mathbf{h}^k , and the lower row shows $\tilde{\mathbf{A}}\mathbf{x}^k$.



(a) $\theta \|\mathbf{h}\|_1$ (b) $\theta \|\mathbf{h}\|_2$ (c) $\theta \|\mathbf{h}\|_1$ (d) $\theta \|\mathbf{h}\|_2$

Fig. 4. (a-b) BPDCAe and (c-d) BPDCA.

30000, and that for AM was 3000 because the subproblems of AM were solved approximately by 10 iterations of FISTA at each iteration. For all methods, the initial points \mathbf{h}^0 and \mathbf{x}^0 are set to be the left and right singular vectors corresponding to the leading singular value of $\mathbf{B}^H \text{diag}(\mathbf{y}) \tilde{\mathbf{A}}$, respectively, which is proposed in [11]. The difference between the objective value at each iteration and those at the ground truth is plotted in Figure 2 in log-scale, where we denoted $\Psi = F + G$ and $\Psi^* := \Psi(\mathbf{h}^*, \mathbf{x}^*)$. As we can see from Figure 2, BPDCAe outperformed the other algorithms: Its convergence was the fastest, and the final objective value $\Psi(\mathbf{h}^k, \mathbf{x}^k)$ was the best. Figure 3 shows the recovered images. Figure 3b shows that there is almost no difference between $\tilde{\mathbf{A}}\mathbf{x}^*$ and $\tilde{\mathbf{A}}\mathbf{x}^k$, while \mathbf{h}^k was not completely recovered. Figures 3b and 3e show that the sequences generated by AM converged to a different stationary point (see also Subsection II-C).

We also solved the deblurring problem with the ℓ_2 regularizer $G(\mathbf{h}, \mathbf{x}) = \theta \|\mathbf{h}\|_2^2$ with $\theta = 0.01$. The comparison between the results from these two regularizers are shown in Figure 4. It shows the superiority of the non-smooth ℓ_1 regularization over the ℓ_2 one, which did not recover the sparse blurring kernel.

IV. CONCLUSION

In blind deconvolution, recovering the original signal and the filter is naturally formulated as a minimization a quartic objective function. While existing first-order methods are not theoretically supported because its differentiable part does not have a Lipschitz continuous gradient, our Bregman proximal DC algorithms efficiently work for this problem. We found an appropriate DC decomposition and kernel generating distance, and we proved the convergence theoretically using them. Our numerical experiments on image deblurring demonstrated

that BPDCAe outperformed other existing algorithms and successfully recovered the original image.

REFERENCES

- [1] A. Ahmed, B. Recht, and J. Romberg. Blind deconvolution using convex programming. *IEEE Transactions on Information Theory*, 60(3):1711–1732, 2014.
- [2] L. Balzano and R. Nowak. Blind calibration of sensor networks. In *Proceedings of the 6th International Conference on Information Processing in Sensor Networks*, pages 79–88, 2007.
- [3] A. Beck and M. Teboulle. A fast iterative shrinkage-thresholding algorithm for linear inverse problems. *SIAM Journal on Imaging Sciences*, 2(1):183–202, 2009.
- [4] J. Bolte, S. Sabach, M. Teboulle, and Y. Vaisbourd. First order methods beyond convexity and Lipschitz gradient continuity with applications to quadratic inverse problems. *SIAM Journal on Optimization*, 28(3):2131–2151, 2018.
- [5] L. M. Bregman. The relaxation method of finding the common point of convex sets and its application to the solution of problems in convex programming. *USSR Computational Mathematics and Mathematical Physics*, 7(3):200–217, 1967.
- [6] T. F. Chan and C. K. Wong. Convergence of the alternating minimization algorithm for blind deconvolution. *Linear Algebra and its Applications*, 316:259–285, 2000.
- [7] J. Chen, R. Lin, H. Wang, J. Meng, H. Zheng, and L. Song. Blind-deconvolution optical-resolution photoacoustic microscopy in vivo. *Optics Express*, 21(6):7316–7327, 2013.
- [8] R. J.-L. Fétick, L. M. Mugnier, T. Fusco, and B. Neichel. Blind deconvolution in astronomy with adaptive optics: the parametric marginal approach. *Monthly Notices of the Royal Astronomical Society*, 496(4):4209–4220, 2020.
- [9] S. M. Jefferies and J. C. Christou. Restoration of astronomical images by iterative blind deconvolution. *The Astrophysical Journal*, 415:862–874, 1993.
- [10] D. Krishnan, T. Tay, and R. Fergus. Blind deconvolution using a normalized sparsity measure. In *Proceedings of the IEEE Conference on Computer Vision and Pattern Recognition 2011*, pages 233–240, 2011.
- [11] X. Li, S. Ling, T. Strohmer, and K. Wei. Rapid, robust, and reliable blind deconvolution via nonconvex optimization. *Applied and Computational Harmonic Analysis*, 47(3):893–934, 2019.
- [12] J. S. Liu and R. Chen. Blind deconvolution via sequential imputations. *Journal of the American Statistical Association*, 90(430):567–576, 1995.
- [13] D. Perrone and P. Favaro. Total variation blind deconvolution: The devil is in the details. In *Proceedings of the IEEE Conference on Computer Vision and Pattern Recognition 2014*, pages 2909–2916, 2014.
- [14] S. Takahashi, M. Fukuda, and M. Tanaka. New Bregman proximal type algorithms for solving DC optimization problems. *arXiv preprint*, arXiv:2105.04873, 2021.
- [15] N. Zhao, Q. Wei, A. Basarab, D. Kouamé, and J.-Y. Tourneret. Blind deconvolution of medical ultrasound images using a parametric model for the point spread function. In *Proceedings of the IEEE International Ultrasonics Symposium 2016*, pages 1–4, 2016.